Available online at www.sciencedirect.com

ScienceDirect

Ceramics International 36 (2010) 1177–1188

CERAMICS INTERNATIONAL

www.elsevier.com/locate/ceramint

Review

Survey on wetting of SiC by molten metals

G.W. Liu [a,b], M.L. Muolo [a], F. Valenza [a], A. Passerone [a,*]

[a] Inst. for Energetics and Interphases, IENI-CNR, Via De Marini 6, 16149 Genoa, Italy
[b] State Key Laboratory for Mechanical Behavior of Materials, Xi'an Jiaotong University, Xi'an 710049, China

Received 2 July 2009; received in revised form 26 November 2009; accepted 16 December 2009
Available online 28 January 2010

Abstract

Good wetting and low reactivity of metal/ceramic couples are key factors in many technological processes, in particular in metal/ceramic joining, to avoid degradation of ceramics and to achieve the desired properties during service. Silicon carbide is a covalent material of great technological interest due to its excellent overall properties. Starting from a survey of the surface energies of SiC and liquid metals, the reactivity and wettability of pure metal/SiC systems, as well as the wetting behavior and mechanisms of (liquid metal + Si)/SiC systems are reviewed for understanding the interfacial bonding and for supporting the development of application-oriented processes like non-reactive brazing. Silicon chemisorption and interactions between the molten alloys and SiC at the metal/substrate interface and the intrinsic properties of the alloys or of the pure metals are considered to play the key roles in interfacial bonding. In particular, additions of Si can limit or even suppress the substrate dissolution leaving the solid–liquid interface nearly undisturbed. At the same time, oxidation–deoxidation processes at the SiC surface are the basic mechanisms to be controlled in order to allow the liquid phases to contact a "pure" SiC surface. The need of further investigations, covering basic interfacial phenomena including both experiments and ab-initio modeling of the solid–liquid interfaces is strongly underlined.

Keywords: A. Joining; B. Interfaces; D. SiC; Wetting

Contents

1. Introduction

Silicon carbide is a covalent material of great technological interest due to its excellent overall properties including good mechanical resistance, high thermal conductivity, good thermal shock behavior, high oxidation and erosion resistances [1]. Its applications are involved in both structural and functional materials. Indeed, it is currently used in the reinforcement of metal–matrix composites, in nuclear plants, for heat exchangers, for optical devices and as the ceramic component of metal/ceramic couples.

Basic studies related to the interactions between metals and ceramics are relevant for all the above-mentioned industrial

---

* Corresponding author. Tel.: +39 010 6475 716; fax: +39 010 6475 700.
E-mail address: a.passerone@ge.ieni.cnr.it (A. Passerone).

0272-8842/$36.00 © 2010 Elsevier Ltd and Techna Group S.r.l. All rights reserved.
doi:10.1016/j.ceramint.2010.01.001

applications, to understand the mechanisms of materials stability and reactivity. These studies are usually performed at high temperature by means of wetting experiments where a liquid metal is put in contact with a solid (ceramic) substrate following one of these techniques: sessile drop [2], dispensed drop [3], transferred drop [4], dip coverage [5], immersion–emersion [6], micro-droplet [7] and pressure infiltration [8–12]. The sessile drop technique is the most frequently used one because of its apparent simplicity, while the pressure infiltration technique is mainly used for wetting between liquid metals and ceramic preforms. Otherwise, a ‘‘solid state wetting technique’’ was put forward by Wang and Wynblatt [13–15]. Actually, the main difference between micro-droplet and solid state wetting techniques lies in the experimental temperature. The metal components used in the two techniques are in the liquid or solid state during the ‘‘wetting’’ process, respectively.

The wettability of a liquid metal on a solid ceramic surface is commonly evaluated by measuring the contact angle θ. Indeed, the contact angle value is related to the bonding quality of the metal/ceramic interface. The macroscopic contact angle θ (measured inside the liquid phase) is defined by Young's equation:

$$\cos\theta = \frac{\sigma_{\mathrm{SV}} - \sigma_{\mathrm{SL}}}{\sigma_{\mathrm{LV}}} \tag{1}$$

where σ_{IJ} denotes the characteristic surface energies of the solid (S)–liquid (L)–vapour (V) system.

The work of adhesion Wa of a metal/ceramic interface is a measure of the interfacial strength at the test temperature. It is defined as:

$$Wa = \sigma_{\mathrm{SV}} + \sigma_{\mathrm{LV}} - \sigma_{\mathrm{SL}} \tag{2}$$

Introducing Eqs. (1) into (2), we obtain the Young–Dupré equation:

$$Wa = \sigma_{\mathrm{LV}}(1 + \cos\theta) \tag{3}$$

From a formal point of view, a liquid phase is considered to wet a solid if $\theta < 90^\circ$.

For a fixed metal/ceramic couple, the wetting behavior can be influenced by many factors: to obtain reliable Young contact angle measurements, some essential parameters, such as the chemical composition of the solid and liquid components, the substrate surface roughness, the characterization of substrate surface chemistry before and after the experiment and the experimental furnace conditions, must be given [2,16,17,33]. Besides temperature and holding time, the atmosphere, especially oxygen partial pressure [18–20], can affect the wetting results (the final or equilibrium contact angle and the spreading kinetics [21,22]). The substrate quality may include surface chemistry state (such as surface oxidation, metallization and even non-stoichiometry [23,24]), surface roughness [25], surface polarity [26] or structure and substrate phase composition (such as surface anisotropy [27], presence of sintering aids [28] and of different phases [29]). In addition, some products often form at the interface due to interfacial reactions during the wetting process, thus the presence of this new interface has to be taken into account. The wetting behavior may be classified into two groups, non-reactive and reactive wetting: non-reactive wetting occurs when a liquid spreads on a surface in the absence of interfacial reactions; on the contrary, when wetting and its kinetics are affected by reactions (true chemical reactions, dissolution, mass transfer, etc.) it is referred to as reactive wetting [29–34].

Due to the non-wetting characteristics of most pure metals on ceramic materials, specific methods for improving the wettability of metals on ceramics have been put forward, involving prior surface treatment and/or addition of active elements. The nature of the two methods is the same and both of them achieve the wetting goal by changing the chemical character of the contact interface. Here, the active element method for improving the wettability is taken into consideration. Indeed, good wetting and low reactivity between liquid metals and ceramics are required, in order to obtain a good adhesion in fabrication processes (metal/ceramic composites, joining, etc.), to avoid degradation of ceramics and to achieve the desired properties during service [1,2]. However, since the active element method belongs to the reactive wetting technique category, it is possible that degradation of ceramics occurs and interfacial reactions provide sources for crack initiation because of brittle products, resulting in deleterious effects on the final mechanical properties of the metal–ceramic couple.

2. Reactivity and wettability of pure metal/SiC systems

2.1. Reactivity of pure metals with SiC

The reactivity of the pure metals with SiC directly affects the interfacial reactions, wetting and bonding. Based on the research results of Kurokawa and Nagasaki [35] and the reviews of Rabin [36] and Li and Zhang [37], the pure metals may be classified into four categories according to their reactivity with SiC, as shown in Table 1. For the first category, there are almost no chemical reactions between the metals and SiC under the experimental conditions. For the second one, only stable silicides can form at the interface; the silicon and carbon originated from SiC matrix tend to diffuse into the metal; the carbon can exist as a solid solution provided the solubility of carbon in the metal is high enough, otherwise it will segregate as graphite in the liquid phase or even at the solid–liquid interface after saturation. For the third one, the carbides are the main products, as most silicon dissolves into the metal and forms carbides, although sometimes silicide can form. Stable ternary carbides can also be found, as in the case of the presence of V: $4\mathrm{SiC} + 14\ \mathrm{V} \rightarrow \mathrm{V}_5\mathrm{Si}_3\mathrm{C}_X + \mathrm{V}_3\mathrm{Si} + 3\ \mathrm{V}_2\mathrm{C}$

Table 1
Reactivity of pure metal/SiC systems [35–37].

Type	Reactivity	Metal
1	No reaction	Au, Ag, Sn, Pb, Ge
2	$\mathrm{Me} + \mathrm{SiC} \rightarrow \mathrm{silicide} + \mathrm{C}$	Ni, Fe, Cu, Co
3	$\mathrm{Me} + \mathrm{SiC} \rightarrow \mathrm{Si} + \mathrm{Carbide}$	V, Al, Nb
4	$\mathrm{Me} + \mathrm{SiC} \rightarrow \mathrm{silicide} + \mathrm{Carbide}$	Zr, Hf, Cr, Ta, W, Ti, Mo

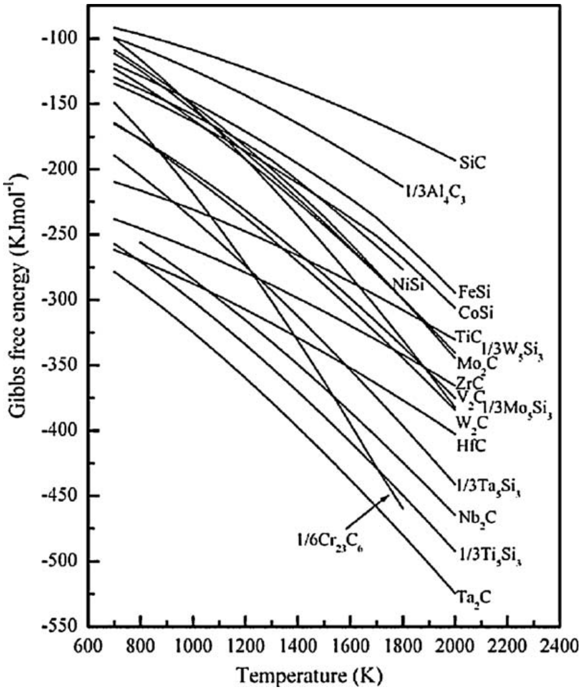

Fig. 1. Gibbs free energies of the formation of SiC and of the main carbides and silicides. The data come from [39] except those of FeSi and V_2C [40].

[38]. For the fourth category, a mixed layer containing silicides and carbides often forms at the interface by reaction and mutual diffusion between the metal and the ceramic.

The Gibbs free energies of formation of SiC and of the main carbides and silicides are shown in Fig. 1. The Al, Fe, Ni and Co reactivity with SiC is low due to the small differences of Gibbs free energy of formation between Al_4C_3, NiSi, FeSi, CoSi and SiC (Fig. 1). On the contrary, some pure metals, such as V, Nb and the metals in the fourth category (Table 1), are called active elements, because they react with SiC giving more stable products, as shown by their Gibbs free energy values (Fig. 1). XC-type carbides of Ti, Zr and Hf are the main reaction products because of their high reactivity resulting from the under filling of their outer electron shell configuration. For those refractory metals, such as Ta, Mo and W, X_2C-type carbides and X_5Si_3-type silicides are the preferred forms. Actually, the interfacial reaction behavior between active elements and SiC is very complicated. For example, for Cr, six compounds ($Cr_{23}C_6$, Cr_7C_3, Cr_3C_2, Cr_3Si, CrSi and Cr_5Si_3C) are detected, and the $Cr_{23}C_6$ phase is the most commonly detected one due to its lowest Gibbs free energy of formation.

2.2. Wettability of pure liquid metals on SiC

The wettability of pure metals on SiC is an important reference for investigating the wetting behavior and mechanism and designing brazing alloys. The contact angle values of pure liquid metals in contact with SiC are listed in Table 2. For each metal, a range of contact angles is given because they are obtained at different temperatures. As shown in Table 2, the non-reactive pure metals Au, Ag, Sn, Pb and Ge when in contact with α-SiC, show non-wetting behavior. However, the values of the contact angles are deeply influenced by the composition of the solid substrate [44]. For example, contact angles of 42° at 1473 K and 0° at 1693 K are reported for Ge when the pure metal is brought in contact with SiC reaction bonded with 10% free silicon (compositions are given in at.% in the whole text). Similarly, almost all the reactive metals (Ni, Co, Fe, Cu and Al) show a large spectrum of contact angles, which can even go through the ''wetting–non-wetting'' transition with temperature raising, i.e. when interfacial reactions become stronger. The contact angle of silicon on SiC is in the range of 30–45°; the wettability of silicon on SiC is usually better than that of all other pure metals.

3. Surface energies of liquid metals and SiC

3.1. Surface energies of liquid metals

The work of adhesion, *Wa*, can be calculated by Eq. (3) using the contact angle (θ) and liquid–vapour surface energy (σ_{LV}) obtained by experiment or calculation. Then, *Wa* can be used to pre-estimate the bonding quality of the ceramic/ceramic or ceramic/metal brazed joints, because the joint mechanical properties depend also on the chemical interfacial bonding between the brazing filler metal and the ceramic component.

The surface energies of some pure liquid metals and their silicon alloys are listed in Table 3. The surface energy of pure liquid metals decreases linearly when temperature increases. The relationship is generally expressed as $\sigma(T) = \sigma_0 + k(T - T_m)$ (where σ_0 is the surface energy at the melting point T_m and $k = (d\sigma/dT)$ is the temperature coefficient). Eustathopoulos et al. [89] calculated the temperature coefficients of surface tension of pure liquid metals, as shown in Table 4, and compared them to the experimental ones [90] when possible. It is observed that the calculated coefficients k are mostly in the range of -0.1 to -0.3 mJ m^{-2} K^{-1} (Table 4). In particular, it can be underlined that the surface energies of liquid Me–Si

Table 2
Contact angles of pure liquid metals on SiC.

Metal	Temp. (K)	θ (°)	Ref.	Metal	Temp. (K)	θ (°)	Ref.
Au	1336–1703	150–110	[41–45]	Fe	1633–1873	70–20	[44,54]
Ag	1233–1473	140–110	[44,49]	Cu	1356–1723	165–30	[45–47,51,55–57]
Sn	505–1473	165–75	[44,45,50,52]	Co	1803	63–55	[44]
Ge	1073–1703	165–90	[43,44]	Pb	603	170–160	[44]
Ge	1473	42	[44]	Al	933–1746	155–30	[6,7,44–46,58–63]
Ge	1573, 1693	0	[44]	Si	1673–1773	54–30	[43,51,64–71]
Ni	1623–1773	86–36	[44,51–53]				

Table 3
Surface energies of pure liquid metals and some of their liquid binary alloys containing Si. Data from different sources for comparison; a critical review can be found in [81]; temperatures in italics refer to the melting point.

Metal (at.%)	Temp. (K)	σ_{LV} (mJ m^{-2})	Ref.	Metal (at.%)	Temp. (K)	σ_{LV} (mJ m^{-2})	Ref.
Au	$T \geq T_m$	$1138–0.19\ (T - T_m)$	[72]	Ni–85Si	1633	740	[82]
Au	*1336*	1150	[71,81]	Fe	*1810*	1880	[81]
Au	$T \geq T_m$	$1115–0.101\ (T - T_m)$	[75]				
Au	1423	1100	[76]	Fe–33.33Si	1633	750	[83]
Au–(0–100)Si	T_m–1723	1150–746	[75]	Fe–66.67Si	1633	750	[83]
Ag	1703	856	[72]	Cu	1373	1250	[52,76]
Ag	*1234*	926	[71,81]	Cu	1473–1773	1288–1228	[77,79]
Ag	1373	900	[76]	Cu	*1357*	1320	[81]
Ag–5Si	1473	880	[49]	Cu	1373	1320	[84,85]
Ag–11Si	1473	860	[49]	Cu–3Si	1373	1240	[71]
Ag–30Si	1473	850	[49]	Cu–10Si	1373	1220	[71]
Sn	1373, 1473	440, 425	[52]	Cu–30Si	1373	1180	[71]
Sn	$T \geq T_m$	$544–0.07\ (T - T_m)$	[73]	Cu–25Si	1423	1050	[66]
Sn	1323	450	[76]	Co	$T \geq T_m$	$1890–0.19\ (T - T_m)$	[86]
Sn	623–1073	536–504	[77]	Co	1823–2043	1594–1530	[77,79]
Sn–(0–100)Si	1723	~450–720	[78]	Pb	$T \geq T_m$	$468–0.13\ (T - T_m)$	[73]
Ge	$T \geq T_m$	$581–0.119\ (T - T_m)$	[72]	Pb	673–973	459–420	[77]
Ge	$T \geq T_m$	$642–0.140\ (T - T_m)$	[71]	Pb	*600*	457	[81]
Ge	1323	620	[76]	Al	1073–1373	~850–780	[58,71,83]
Ni	1740–1953	1750–1690	[77,79]	Al	*933*	914	[73]
Ni	$T \geq T_m$	$1823–0.46\ (T - T_m)$	[80]	Si	$T \geq T_m$	$754–0.062\ (T - T_m)$	[73,74]
Ni	*1728*	1795	[81]	Si	$T \geq T_m$	$746–0.152\ (T - T_m)$	[49]
Ni–40Si	1633	1320	[82]				
Ni–50Si	1633	1080	[82]	Si	1633	720	[82]
Ni–67Si	1633	850	[82]	Si	1703–1753	~800	[67,87,88]

alloys, at constant temperature, decrease when the silicon content increases if $\sigma_{Me} > \sigma_{Si}$; in the case of alloys like the Sn–Si alloys, the surface energy increases with Si content increasing because the surface energy of Sn is lower than that of Si. Actually, high surface tensions are associated with prominent electron bonding, which in turn means that some relationship between σ_{LV} at T_m and the melting temperature should be expected. This is indeed true, and the highest surface energy values are generally found in high-melting point metals [91]. So, the work of adhesion of some binary Me–Si alloys can be moderately improved by adding one or several of these elements, under the condition that the contact angle keeps

Table 4
Experimental and calculated values of $d\sigma/dT$ for pure liquid metals [89,90].

Element	$d\sigma/dT$ (mJ m^{-2} K^{-1})		Element	$d\sigma/dT$ (mJ m^{-2} K^{-1})		Element	$d\sigma/dT$ (mJ m^{-2} K^{-1})	
	Experimental	Calculated		Experimental	Calculated		Experimental	Calculated
Ag	−0.17	–	Lu	−0.07	−0.21	Sn	−0.11	–
Al	−0.15	–	Mg	−0.15	−0.16	Sr	−.075	–
Au	−0.19	–	Mn	−0.35	−0.23	Ta	–	−0.24
Ba	−0.07	−0.06	Mo	–	−0.23	Tb	−0.06	−0.16
Be	–	−0.25	Nb	–	−0.19	Th	–	−0.14
Cd	−0.20	−0.16	Nd	−0.09	−0.11	Ti	–	−0.28
Ce	−0.07	−0.09	Ni	−0.42	–	U	−0.14	−0.16
Co	−0.37	–	Os	–	−0.29	V	–	−0.26
Cr	−0.20	−0.33	Pb	−0.11	–	W	–	−0.20
Cu	−0.19	–	Pd	−0.28	−0.24	Y	−0.09	−0.11
Dy	−0.13	−0.15	Pr	−0.09	−0.14	Yb	−0.10	−0.17
Er	−0.12	−0.16	Pt	–	−0.29	Zn	−0.25	−0.22
Eu	−0.05	−0.16	Pu	–	−0.13	Zr	–	−0.19
Fe	−0.23	−0.29	Rb	−0.07	−0.05			
Ga	−0.07	–	Re	–	−0.21			
Ge	−0.105	–	Rh	–	−0.24			
Hf	–	−0.19	Ru	–	−0.28			
Hg	−0.215	–	Sb	−0.04	−0.10			
In	−0.12	–	Sc	−0.12	−0.21			
Ir	–	−0.18	Si	−0.48	−0.19			
Li	−0.16	−0.14	Sm	−0.07	−0.10			

Table 5
Calculated unrelaxed and relaxed energies for β-SiC surfaces [95].

Crystal surface	σ_{SV} (mJ m^{-2}) unrelaxed	σ_{SV} (mJ m^{-2}) relaxed
β-SiC (1 0 0)	5275	4658
β-SiC $(\bar{1}\,0\,0)$	4818	1908
β-SiC (1 1 1)	2584	1767
β-SiC $(\bar{1}\,\bar{1}\,\bar{1})$	2446	718.4
β-SiC (1 1 0)	3236	2330

almost constant; in this case, such addition, due to the increase of σ_{LV}, can improve the interfacial bonding quality (Eq. (3)).

3.2. Surface energy of SiC

In principle, we can calculate the solid–liquid interfacial energies σ_{SL} of alloy/SiC systems by Eq. (1) or (2) by using the experimental or calculated values of the metal surface energies σ_{LV}, their contact angle θ and the surface energy σ_{SV} of SiC [92]. However, only calculated values of the surface energy of SiC σ_{SV}(SiC) are available. Firstly, Bruce [93] gave the surface energy as a function of temperature for the (1 1 1) plane of β-SiC (3000–0.546T, $T \geq 0$). Then, Oshcherin [94] calculated surface energy values of 2700, 1620 and 2180 mJ m^{-2} at room temperature for the (0 0 0 1) Si-terminated surface of α-SiC, $(0\,0\,0\,\bar{1})$ C-terminated surface of α-SiC and the (1 1 1) plane of β-SiC, respectively. Takai et al. [95] calculated the surface energies of various crystallographic planes of β-SiC by employing a semi-empirical potential energy in association with a Monte Carlo simulation technique. They obtained a series of relaxed and unrelaxed surface energies (Table 5); however, having ignored the charge transfer forces, they declared that these values can be only used for qualitative comparisons. According to Refs. [79–81], the values of σ_{SV}(SiC) strongly depend on temperature, crystal structure, crystal surface polarity, etc. The commonly used SiC materials, such as reaction bonded SiC (RB-SiC), pressureless sintered SiC (PLS-SiC), hot pressed SiC (HP-SiC), hot isostatic pressed SiC (HIP-SiC), recrystallized SiC (RC-SiC) and single crystals (α-SiC or β-SiC), have different crystal structure, surface polarity and bulk composition with a consequent scatter in the σ_{SV}(SiC) values [83]. Some authors [13,51] adopted 1800 mJ m^{-2} for the value of α-SiC, based on the similar configuration of the α-SiC (0 0 0 1) and the β-SiC (1 1 1) surfaces.

4. Wetting behavior and mechanisms

The elemental silicon readily wets ($\theta \approx 30$–45°) SiC substrates (Table 2). Recent investigations have shown that some binary silicon alloys or silicides can also present good non-reactive wetting on SiC surface. In the following Sections 4.1–4.3, the reactivity of pure metals with SiC and the wetting characteristics of their binary alloys with Si on SiC are classified and summarized.

4.1. Non-reactive pure metal + Si/SiC systems

The wettability of non-reactive alloy (non-reactive pure metal with additions of Si)/SiC systems is listed in Table 6. The Au–Si/SiC system was investigated at 1373 K [96]. The authors found contact angles less than 20° at $X_{Si} \approx 0.4$ (lower than that of Si/SiC system) when using a molybdenum furnace (Fig. 2), whereas it was close to 0° when using an alumina furnace with $X_{Si} \approx 0.3$. The same authors argued that the good wetting and adhesion were due to silicon chemisorption at the metal/SiC interface with the formation of strong covalent-like bonds between Si and SiC. On another hand, Naidich et al. [42] investigating the influence of silicon content and temperature

Table 6
Contact angles of non-reactive alloys: (non-reactive pure metal + Si)/SiC systems.

Metal (at.%)	Substrate character Structure, roughness, etc.	Temp. (K)	Atmosphere	θ (°)	Ref.
Au–40Si	6H–SiC, (0 0 0 1), R = 1.5 nm	1373	10^{-2} Pa, $P_{O_2} = 10^{-2}$ Pa molybdenum furnace	in Fig. 2	[96]
Au–(31 ± 1)Si	6H–SiC, (0 0 0 1), R = 1.5 nm	1373	10^{-2} Pa, $P_{O_2} = 10^{-2}$ Pa graphite furnace	59	[96]
Au–(31 ± 1)Si	6H–SiC, (0 0 0 1), R = 1.5 nm	1373	10^{-2} Pa, $P_{O_2} = 10^{-2}$ Pa alumina + graphite tube	30	[96]
Au–(31 ± 1)Si	6H–SiC, (0 0 0 1), R = 1.5;nm	1373	10^{-2} Pa, $P_{O_2} = 10^{-2}$ Pa alumina furnace	0	[96]
Au–10Si	6H–SiC, (0 0 0 1), mixed C–Si-face, $R \approx 10$ nm	1573	Purified Ar	15	[42]
Au–10Si	6H–SiC, (0 0 0 1), mixed C–Si-face, $R \approx 10$ nm	1773	Purified Ar	7	[42]
Au–18.5Si	6H–SiC, (0 0 0 1), mixed C–Si-face, $R \approx 10$ nm	1373	Purified Ar	12	[42]
Au–60Si	6H–SiC, (0 0 0 1), mixed C-Si-face, $R \approx 10$ nm	1373	Purified Ar	20	[42]
Au–60Si	6H–SiC, (0 0 0 1), mixed C–Si–face, $R \approx 10$ nm	1423	Purified Ar	17	[42]
Au–60Si	6H–SiC, (0 0 0 1), mixed C–Si-face, $R \approx 10$ nm	1473	Purified Ar	15	[42]
Au–60Si	6H–SiC, (0 0 0 1), mixed C–Si-face, $R \approx 10$ nm	1723	Purified Ar	12	[42]
Au–60Si	6H–SiC, (0 0 0 1), mixed C–Si-face, $R \approx 10$ nm	1773	Purified Ar	12	[42]
Ag–10Si	6H–SiC, c-axis direction, R = 0.04 μm	1273–1703	Purified Ar	~45	[47]
Ag–5Si	6H–SiC, {0 0 0 1}, Si-face, R = 1–2 nm	1473	Purified He	36	[49]
Ag–11Si	6H–SiC, {0 0 0 1}, Si-face, R = 1–2 nm	1473	Purified He	39	[49]
Ag–30Si	6H–SiC, {0 0 0 1}, Si-face, R = 1–2 nm	1473	Purified He	42	[49]
Sn–0.4Si	HD-α-SiC,	1583	Flowing Ar	~60	[50]
Sn-0.4Si	HD-α-SiC	1773	Flowing Ar	~50	[50]
Sn-17.9Si	HD-α-SiC	1600	Flowing Ar	35	[50]
Sn-17.9Si	HD-α-SiC	1673	Flowing Ar	35	[50]

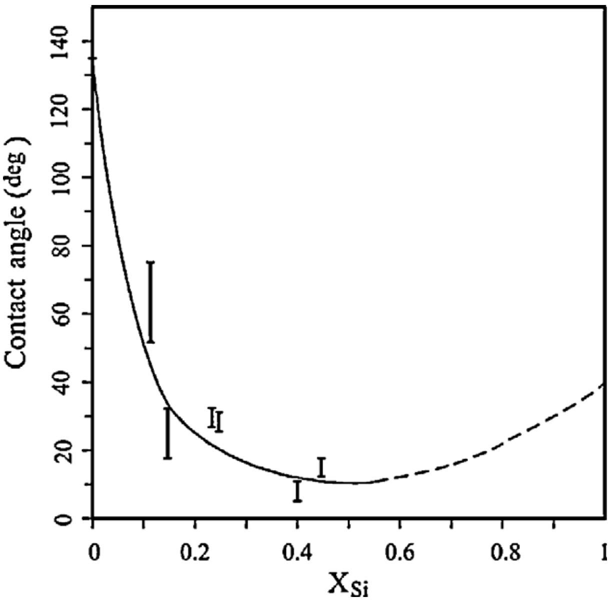

Fig. 2. Variation of contact angle of Au–Si alloys on SiC as a function of Si mole fraction in the melt at 1373 K [96].

on the wetting of Au–Si/SiC system, obtained contact angles, at temperatures ranging from 1373 to 1773 K, varying as a function of Si content, with pronounced minima at about 5° at 1500 °C for $X_{Si} \approx 0.3$. The addition of Au, which surface tension is much higher than the Si surface tension ($\sigma_{Au} = 1070$ mJ m^{-2}, $\sigma_{Si} = 735$ mJ m^{-2} at 1773 K [42]) cannot explain this change. Indeed, these authors attributed the presence of a minimum in the contact angle to the electronic interactions between Au and Si atoms with the SiC substrate: Au–Si interactions in the liquid phase should strengthen the Si–SiC bonds with a transition of valence electrons towards Si atoms. Thus, more-covalent bonds can be established between Si atoms in the alloy and those in the substrate, leading, as a result, to an increased wettability.

For the Ag–Si/SiC system, Li [47] firstly investigated the wettability of Ag–10Si on SiC at 1273–1703 K ($\theta_F \approx 45°$) (Table 6), and found that an addition of 10%Si suppresses the dissolution of silicon carbide without leading to wetting–dewetting phenomena. This result would support the viewpoint of silicon chemisorption at the interface. Subsequently, Rado et al. [48–49] investigated the wetting of Ag–Si/SiC system and found that contact angle values increased from 36° to 42° at 1473 K when Si content varied from 5 to 30 at.%. They considered that the non-reactive wetting and adhesion behavior of Ag–Si/SiC was not due to the silicon chemisorption but to the high adhesion energy of Ag itself on SiC. They suggested that the intrinsic adhesion of Ag (and other similar metals like Au) is not provided by van der Waals interactions but by strong chemical bonds, and evidenced that silicon actually dissolves the wetting barriers of thin layers of SiO_2 or graphite formed on SiC. The related chemical reactions may be expressed as follows:

$$SiO_2\,(s) + Si\,(l) \rightarrow 2SiO\,(g)\uparrow \tag{4}$$

$$SiC\,(s) \Leftrightarrow Si\,(l) + C_{gr} \tag{5}$$

Table 7
Contact angles of non-reactive alloys: (reactive pure metal + Si)/SiC systems.

Metal (at.%)	Substrate character Structure, roughness, etc.	Temp. (K)	Atmosphere	θ (°)	Ref.
Fe–66.67Si	6H–SiC, (0 0 0 1), $R < 20$ nm	1633	10^{-5} to 10^{-4} Pa	30	[54]
Ni–47Si	HD-α-SiC	1773	Flowing Ar	36	[50]
Ni–40Si	6H–SiC, (0 0 0 1), Si-face, $R = 1–2$ nm	1633	10^{-5} to 10^{-4} Pa	21	[1]
Ni–50Si	6H–SiC, (0 0 0 1), Si-face, $R = 1–2$ nm	1633	10^{-5} to 10^{-4} Pa	19.5	[1]
Ni–67Si	6H–SiC, (0 0 0 1), Si-face, $R = 1–2$ nm	1633	10^{-5} to 10^{-4} Pa	31	[1]
Ni–85Si	6H–SiC, (0 0 0 1), Si-face, $R = 1–2$ nm	1633	10^{-5} to 10^{-4} Pa	30.5	[1]
Ni–56Si	HIP-SiC, $R = 20$ nm	1623	3×10^{-4} Pa	23	[98]
Ni–56Si	HIP-SiC, $R = 20$ nm	1623	Static Ar + 5%H_2, 10^5 Pa	23	[98]
Ni–56Si	HIP-SiC, $R = 20$ nm	1473	3×10^{-4} Pa	55	[98]
Ni–56Si	HIP-SiC, $R = 20$ nm	1473	static Ar + 5%H_2, 10^5 Pa	50	[98]
Ni–56Si	HIP-SiC, $R = 20$ nm	1373	3×10^{-4} Pa	48	[98]
Cu–10Si	6H–SiC	1373	1.3–4 × 10^{-3} Pa	42	[56]
Cu–30Si	6H–SiC	1373	1.3–4 × 10^{-3} Pa	33	[56]
Cu–24Si	6H–SiC, (0 0 0 1), $R = 2$ nm	1473	10^{-3} to 10^{-4} Pa	~30	[99]
Cu–24Si	6H–SiC, (0 0 0 1), $R = 2$ nm	1573	Ar	~30	[99]
Cu–25Si	6H–SiC, (0 0 0 1), $R < 20$ nm	1423	10^{-3} Pa	30	[100]
Cu–40Si	6H–SiC, (0 0 0 1), $R < 20$ nm	1423	10^{-3} Pa	36	[100]
Cu–50Si	6H–SiC, (0 0 0 1), $R < 20$ nm	1423	10^{-3} Pa	39	[100]
Cu–40Si	6H–SiC, 60–70 nm SiO_2, (0 0 0 1), C-face, $R = 1–2$ nm	1435	10^{-5} Pa	46	[3]
Cu–40Si	6H–SiC, ~20 nm SiO_2, (0 0 0 1), C-face, $R = 1–2$ nm	1430	10^{-5} P	37	[3]
Cu–20Si	6H–SiC, (0 0 0 1), Si-face, $R = 2$ nm	1423	10^{-3} Pa	32	[101]
Cu–24Si	6H–SiC, (0 0 0 1), Si-face, $R = 2$ nm	1423	10^{-3} Pa	34	[101]
Cu–25Si	6H–SiC, (0 0 0 1), Si-face, $R = 2$ nm	1363	10^{-3} Pa	33	[101]
Cu–30Si	6H–SiC, (0 0 0 1), Si-face, $R = 2$ nm	1423	10^{-3} Pa	38	[101]
Cu–40Si	6H–SiC, (0 0 0 1), Si-face, $R = 2$ nm	1423	10^{-3} Pa	40	[101]
Cu–50Si	6H–SiC, (0 0 0 1), Si-face, $R = 2$ nm	1423	10^{-3} Pa	41.5	[101]
Cu–36Si	β-SiC	1423	6.7×10^{-4} Pa	65	[102]

Neither dissolution of SiC nor micro-cracks was found at the interface and in the bulk phases due to the good ductility of Ag and the low silicon content (5–10%).

Similar conclusions were found for the Sn–Si/SiC system by Tsoga et al. [50]. They demonstrated that additions of silicon into Sn decrease the temperature of the transition between passive and active oxidation of the SiC substrate (passive oxidation means formation of a protective SiO_2 layer at the SiC surface) and, at the same time, improve the wettability by Si adsorption at the liquid–solid interface, thus decreasing the interfacial energy, with final contact angles of about 122°, 62° and 53° at 1333, 1583 and 1773 K, respectively for a Sn–0.4Si alloy and 35° for a Sn–17.9Si alloy at 1673 K.

4.2. Reactive pure metal + Si/SiC systems

The wettability of SiC by non-reactive alloys made of pure metals with Si additions, is listed in Table 7. For the Fe–Si/SiC system, Kalogeropoulou et al. [54] found that when using different atomic ratios (1:0, 2:1 and 1:2) of Fe to Si, the contact angle decreased from 50°, 35° to 30° and that the wetting behavior went from strong reactive, low reactive to non-reactive wetting in turn. These results led them to agree with the mechanism of silicon chemisorption at the Fe–Si/SiC interface.

For the Ni–Si/SiC system, Tsoga et al. [50] found that, at 1773 K and under flowing Ar, the additions of silicon into the nickel matrix (at 2.1, 37.1 and 47.3%) progressively weakened the interfacial reaction between Ni and SiC and promoted the wettability. Only the alloy with a silicon content of 47.3% could maintain non-reactive wetting. Indeed they found that, at low Si content, the Ni atoms react with SiC to form silicon rich phases and carbon, resulting in graphite precipitation. According to the Ni–Si–C ternary phase diagram (Fig. 3) [97], the additions of Si (≥37%) to Ni can suppress the graphite formation at around 1800 K and spreading can occur at a nearly non-reactive alloy/SiC interface (see, for example the A-SiC line in Fig. 3). This point has been further clarified by Rado et al. [1]. They drew the conclusions that, at 1633 K, pure Ni reacts strongly with SiC and that additions of Si to Ni can suppress graphite formation for $X_{Si} > 0.37$: non-reactive Ni–Si alloys can wet well SiC (Fig. 4) The low equilibrium contact angles (20–40°) have been attributed to strong interfacial chemical interactions, while the decrease of contact angle (with the parallel increase of the work of adhesion) in the range of $0 < X_{Ni} < 0.60$ was attributed to the role of Ni d-orbitals which, through a strong hybridization of s–p states of SiC surface, give rise to a high adhesion energy and to the final good wetting found experimentally. Recently, based on a detailed investigations on wetting and spreading kinetics of Ni–56Si/SiC system, Liu et al. [98] confirmed the non-reactive wetting characteristics of Ni–Si/SiC system (Fig. 5) and the combined effects of both temperature and atmosphere on the wetting and spreading processes; in particular, it was possible to confirm that the spreading mechanism at lower temperature (1373 K) is different from that at higher temperatures (1473 and 1623 K) (Fig. 6), due to the fact that the spreading kinetics of non-reactive alloy/SiC systems is mainly controlled by the kinetics of removing of wetting barriers (SiO_2) on the SiC surface due to the formation of SiO through the reaction (4).

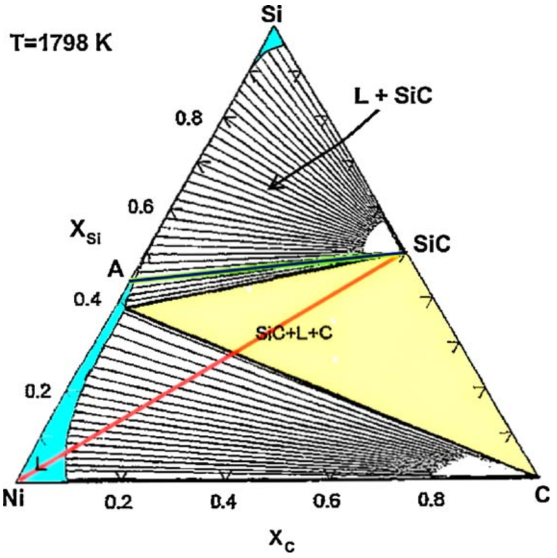

Fig. 3. Schematic isothermal section of Ni–Si–C ternary phase diagram at 1798 K [97].

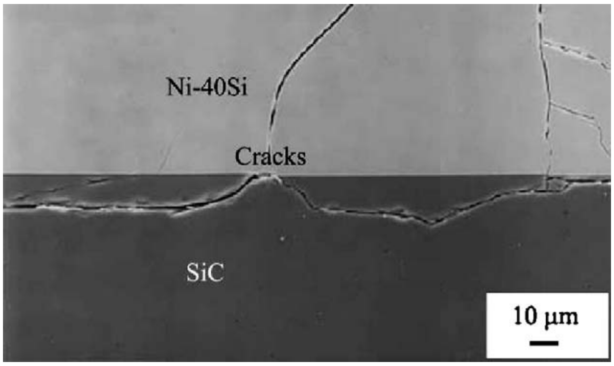

Fig. 4. SEM micrograph of a cross-section in a Ni–40Si/SiC specimen, showing a smooth interface without any graphite precipitates and some cracks formed during cooling. Adapted from [1].

For the Cu–Si/SiC system (Table 7), the contact angles of Cu–Si alloys with (10–50)% Si on SiC are in the range of 30–45° (excepted the 65° of β-SiC) at T between 1363 and 1573 K. These angles correspond to that of Si/SiC. According to Ref. [56], under the conditions $P \sim 10^{-3}$ Pa and $T = 1373$ K, the addition of a small amount of silicon (∼3%) can suppress the formation of interfacial intermediate phases but does not lead to the wetting of SiC. However, the Cu–10Si and Cu–30Si alloys wet the substrate without formation of any intermediate phases. Gasse et al. [99] investigated the influence of the atmosphere on the wettability of 6H–SiC by non-reactive Cu–24Si alloys, and they found a wetting–dewetting transition (from $\theta < 90°$ to $\theta > 90°$) during a thermal cycle between 1200 and 1473 K under argon, which has been attributed to the presence of surface oxidation–deoxidation phenomena occurring during the heating–cooling stages as a function of the oxygen partial pressure in the experimental chamber. Moreover, it has been confirmed that the presence of Si in the Cu matrix can lead to the surface cleaning through the reaction (4), provided the oxygen partial pressure is sufficiently low. Landry et al. [100] found that further additions of silicon

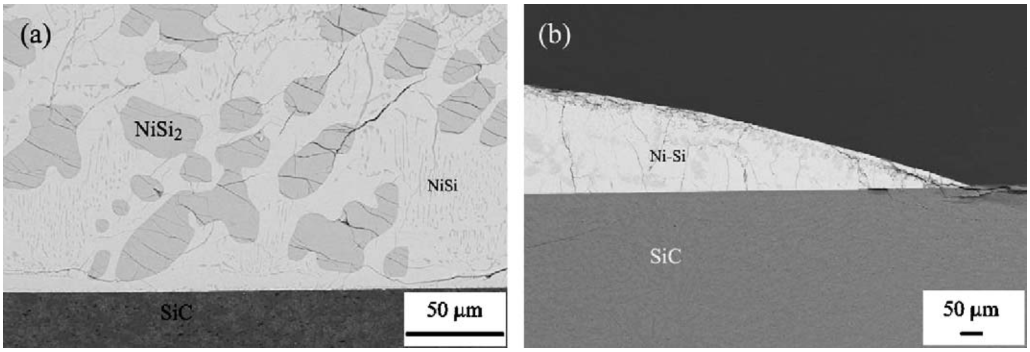

Fig. 5. Cross-section SEM micrographs of the Ni–56Si/SiC couples: (a) 1373 K and (b) a region close to the triple line at 1623 K, showing non-reactive wetting characteristics. The white and gray phases in the drop are NiSi and $NiSi_2$, respectively [98].

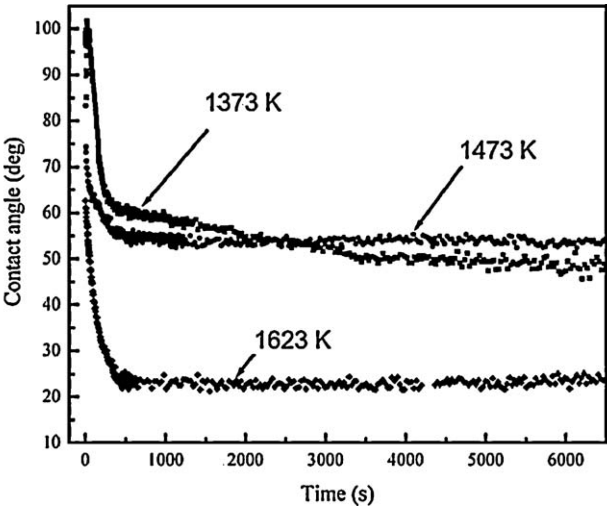

Fig. 6. Contact angle as a function of time. Spreading kinetics of Ni–56Si on SiC at three temperatures in vacuum, showing the effects of temperature on wettability and spreading process and different spreading mechanisms [98].

above 25% have no significant influence on the final contact angle but can inhibit any reactivity between the molten Cu and SiC. They suggest that Si affects the spreading kinetics by controlling the deoxidation of the alloy and of the SiC surface, and that the good wetting in the Cu–Si/SiC systems can be explained by the adsorption of silicon at the Cu/SiC interface. According to Ref. [3] in the Cu–Si/oxidized SiC system, silicon can clean in situ the substrate surface by reaction (4), making the spreading process to take place in three stages: a rapid spreading stage towards a stationary configuration (with constant θ) and a final stage with a constant spreading rate. Such a spreading behavior was interpreted as due to a dissolution–diffusion–evaporation process occurring in the vicinity of the triple line: the oxide layer dissolves into the alloy, then dissolved oxygen diffuses from the oxide/alloy interface to the adjacent liquid/vapour surface and evaporates as SiO. Rado and Eustathopoulos [101] investigated the spreading of Cu–Si alloys on α-SiC single crystal for studying the difference of spreading time between non-reactive silicide/SiC systems and typical non-reactive metal/ceramic systems. They found that the spreading kinetics of non-reactive silicide/SiC systems were controlled by the kinetics of removing the wetting barriers from the SiC surface, mainly through reactions (5) and (6):

$$SiC\,(s) + 2SiO_2\,(s) \Leftrightarrow 3SiO\,(g)\uparrow + CO\,(g)\uparrow \qquad (6)$$

4.3. *Si-rich alloys or silicide/SiC systems*

The contact angles of silicon alloys and silicides on SiC are listed in Table 8. According to Ref. [67], the contact angles of

Table 8
Contact angles of silicon alloys and silicides in contact with SiC.

Metal (at.%)	Substrate	Temp. (K)	Atmosphere	θ (°)	Ref.
Si–(1B,1Cu,1Fe,10Cu, 10Fe)	SB-SiC, HP-SiC	1699	$<1.3 \times 10^{-2}$ Pa	~40	[67]
Si–1Fe	SB-SiC, HP-SiC	1755	$<1.3 \times 10^{-2}$ Pa	28, 37	[67]
Si–10Fe	SB-SiC, HP-SiC	1755	$<1.3 \times 10^{-2}$ Pa	20, 37	[67]
Si–1Cu	SB-SiC, HP-SiC	1755	$<1.3 \times 10^{-2}$ Pa	34, 36	[67]
Si–10Cu	SB-SiC, HP-SiC	1755	$<1.3 \times 10^{-2}$ Pa	28, 45	[67]
Si-1B	SB-SiC, HP-SiC	1755	$<1.3 \times 10^{-2}$ Pa	26, 40	[67]
FeSi	6H–SiC	1693	Vacuum	<40	[70]
Fe_2Si_5	6H–SiC	1623	Vacuum	<40	[70]
CoSi	6H–SiC	1773	Vacuum	<40	[70]
$CoSi_3$	6H–SiC	1673	Vacuum	60	[70]
$TiSi_2$	6H–SiC	1773	Vacuum	<40	[70]
Cr_3Si_2	6H–SiC	1733	Vacuum	<40	[70]
Si–27.5Co	PLS-SiC	1623	Ar, P_{O_2}: <5, 10, 100 ppm	~40	[103]
Si–27.5Co	PLS-SiC	1623	Ar, P_{O_2}: 100, 300 ppm	~45	[103]
Si–27.5Co	PLS-SiC	1623	Ar, P_{O_2}: 300 ppm	~60	[103]

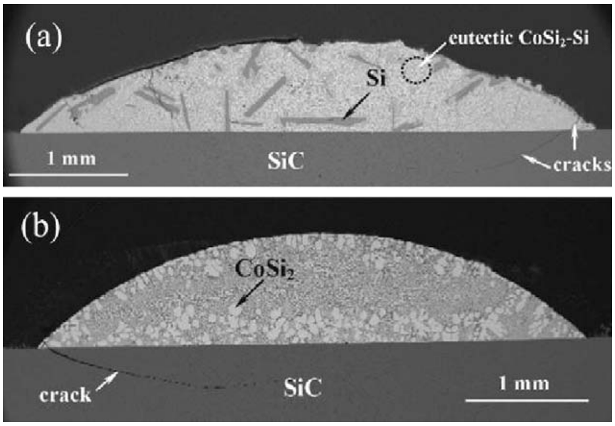

Fig. 7. (a) SEM image of a cross-section of a Si–27.5Co alloy on SiC under pure Ar; (b) SEM image of a cross-section of a Si–27.5Co alloy on SiC under Ar—300 ppm O_2 mixture introduced at melting; showing no reactivity at the interface and some cracks in the drop and substrate. Adapted from [103].

the silicon alloys containing Fe, Cu or B on self-bonded (SB) SiC are slightly lower than those on HP-SiC at 1755 K due to the difference of substrate surface structure (roughness or porosity), and the contact angles on HP-SiC are similar to that of Si/SiC. Furthermore, according to Ref. [70], most silicides ($CoSi_3$ excepted) in contact with 6H-SiC show good wetting with contact angle values $<40^\circ$.

Recently, Mailliart et al. [103] investigated the influence of the oxygen partial pressure on wetting in the Si–27.5Co/SiC system and the relationship between wetting and deoxidation of SiC surfaces in a temperature range up to 1623 K. They obtained final contact angles of 40–60° (Table 8), and found that no reaction underwent at the alloy/ceramic interface and that some cracks were present only in the solidified drop and substrate but not at the interface (Fig. 7). They concluded that the wetting in a system where both the SiC substrate and the liquid Si–Co alloy are oxidizable materials, depends on the surface condition of the liquid alloy, and that clean and oxide-free surface would promote wetting. The formation of a clean liquid surface critically depends on the type of surface oxidation, which could be active or passive, as a function of the P_{O_2}: the transition from the passive to the active process, which takes place at a definite temperature function of P_{O_2}, leads to clean, oxide-free liquid alloy promoting SiC deoxidation and good wetting and adhesion.

5. Summary

The wettability of SiC has been shown to depend on three main factors:

(1) the condition of the SiC surface;
(2) the presence of adsorption phenomena at the solid–liquid interface;
(3) the presence of reaction/dissolution phenomena between the liquid phase and the solid substrate.

The presence of a SiO_2 layer at the SiC external surface prevents wetting and adhesion. Thus, experimental or processing conditions should be chosen where this surface layer can be eliminated. This can be obtained by fixing an oxygen partial pressure for which the transition between passive (formation of SiO_2) to active (formation of SiO) oxidation takes place (in the cases reported here $T \approx 1600$ K). But, on the other hand, the SiO_2 surface layer can also be eliminated through reaction (4), by adding Si to the molten alloy. In both cases, wetting can occur on a clean SiC surface.

However, an additional difference still exists, because metals and alloys can be classified as non-reacting and reacting with SiC. In the first case, the good wetting and adhesion on clean SiC surfaces are attributed to silicon chemisorption at the metal/SiC interface with the formation of strong covalent-like bonds between Si and SiC, to the electronic properties of these alloys and to their interaction with SiC, as well as the high adhesion energy of the pure metal itself on SiC. This is the case of the binary Si alloys (such as Au–Si, Ag–Si, Cu–Si,) within a limited silicon content on SiC. Among these alloys, Au–Si shows the best wetting behavior ($\theta \approx 10$–20°). For the ‘‘relatively’’ non-reactive wetting alloys (reactive pure metal + Si)/SiC systems, it has been shown that Si plays a key role in determining the solid–liquid behavior. Indeed, pure metals like Ni, Co, Fe, etc. when put in contact with SiC react with it and dissolve a large amount of Si and C into the liquid phase. This is supported by the ternary phase diagrams X–Si–C. In all cases, it is seen that the tie-line between the pure metal X and the SiC compound crosses inevitably the SiC + C + liquid region, which means that both dissolution of the substrate and reprecipitation of C takes place. However, the same diagrams show that additions of Si from $X_{Si} \approx 0.3$ upward can limit or even suppress the substrate dissolution leaving only two phases at equilibrium, i.e. the nearly pure X–Si alloy and the solid SiC. It is thus clear that ternary Me–Si–C phase diagrams should be established for a larger number of systems with a wider access to their isothermal sections related to the experimental temperatures.

From the large amount of experimental results and from their thermodynamic interpretation, it appears clearly that the adhesion between liquid metals and SiC is mainly due to two kinds of chemical bonds: those at the metal–carbide interface and the metal–metal ones. An efficient way to study these interactions and to quantify their effects in terms of adhesion energy is offered by modeling, through molecular dynamics approaches or by applying the Density Functional Theory (DFT) [89–92,104–107]. Up to now, most efforts have been made to model metal/oxides interfaces, but a few calculations exist on metal/SiC systems, arriving at a correct estimation of the metal–ceramic bonding mechanisms [108]. In recent years, an increasing effort is being made to model metal/ceramic systems through DFT [19,109,110] which seems to open new important insights into the basic solid–liquid interactions at high temperatures.

From the applications point of view, it should be noted that the Ni–Si alloys possess the best wettability ($\theta \approx 20$–30°) and the greater potential for joining SiC ceramics. Indeed, as it has been shown, Si contents larger than about $X_{Si} = 0.4$ lead to unreacted interfaces, with very few cracks and defects. The design and development the NiSi based non-reactive brazing alloys is highly promising for joining SiC or its composites, provided the addition of alloying elements is taken into account in order to improve their toughness and high temperature performances.

References

[1] C. Rado, S. Kalogeropoulou, N. Eustathopoulos, Wetting and bonding of Ni–Si alloys on silicon carbide, Acta Mater. 47 (2) (1999) 461–473.

[2] N. Eustathopoulos, M.G. Nicholas, B. Drevet, Wettability at High Temperature, Elsevier, Amsterdam, 1999.

[3] O. Dezellus, F. Hodaj, C. Rado, J.N. Barbier, N. Eustathopoulos, Spreading of Cu–Si alloys on oxidized SiC in vacuum: experimental results and modelling, Acta Mater. 50 (5) (2002) 979–991.

[4] R. Voitovitch, A. Mortensen, F. Hodaj, N. Eustathopoulos, Diffusion-limited reactive wetting: study of spreading kinetics of Cu–Cr alloy on carbon substrates, Acta Mater. 47 (4) (1999) 1117–1128.

[5] T. Choh, T. Oki, Wettability of SiC to aluminium and aluminium alloys, Mater. Sci. Technol. 3 (55) (1987) 378–385.

[6] V. Laurent, D. Chatain, N. Eustathopoulos, Wettability of SiO_2 and oxidized SiC by aluminium, Mater. Sci. Eng. A 135 (1991) 89–94.

[7] A.C. Ferro, B. Derby, Development of a micro-droplet technique for wettability studies: application to Al–Si/SiC system, Scripta Metall. Mater. 33 (5) (1995) 837–842.

[8] S.Y. Oh, J.A. Cornie, K.C. Russell, Wetting of ceramic particulates with liquid aluminium alloy. Part II. Study of wettability, Metall. Trans. A 20 (3) (1989) 533–541.

[9] J.M. Molina, J. Tian, C. Garcia-Cordovilla, E. Louis, J. Narciso, Wettability in pressure infiltration of SiC and oxidized SiC particle compacts by molten Al and Al–12 wt% Si alloy, J. Mater. Res. 22 (8) (2007) 2273–2278.

[10] R. Voytovych, V. Bougiouri, N.R. Calderon, J. Narciso, N. Eustathopoulos, Reactive infiltration of porous graphite by NiSi alloys, Acta Mater. 56 (10) (2008) 2237–2246.

[11] M. Kida, M. Bahraini, J.M. Molina, L. Weber, A. Mortensen, High-temperature wettability of aluminum nitride during liquid metal infiltration, Mater. Sci. Eng. A 495 (1–2) (2008) 197–202.

[12] V. Michaud, A. Mortensen, On measuring wettability in infiltration processing, Scripta Mater. 56 (10) (2007) 859–862.

[13] Z. Wang, P. Wynblatt, Wetting and energetics of solid Au and Au–Ge/SiC interfaces, Acta Mater. 46 (14) (1998) 4853–4859.

[14] Z. Wang, P. Wynblatt, Alloying effects of Sn and Si on wetting and energetics of solid Au/SiC interfaces, Mater. Sci. Eng. A 259 (2) (1999) 287–295.

[15] P. Wynblatt, The effects of interfacial segregation on wetting in solid metal-on-metal and metal-on-ceramic systems, Acta Mater. 48 (18–19) (2000) 4439–4447.

[16] N. Eustathopoulos, N. Sobczak, A. Passerone, K. Nogi, Measurement of contact angle and work of adhesion at high temperature, J. Mater. Sci. 40 (9–10) (2005) 2271–2280.

[17] G. Levi, W.D. Kaplan, Aluminium–alumina interface morphology and thermodynamics from dewetting experiments, Acta Mater. 51 (2003) 2793–2802.

[18] E. Saiz, R.M. Cannon, A.P. Tomsia, High temperature wetting and the work of adhesion in metal/oxide systems, Annu. Rev. Mater. Res. 38 (2008) 197–226.

[19] M.L. Muolo, F. Valenza, A. Passerone, D. Passerone, Oxygen influence on ceramics wettability by liquid metals: experiments and modelling, J. Mater. Sci. Eng. A 495 (2008) 153–158.

[20] E. Arato, P. Costa, E. Ricci, Oxygen transport phenomena at the liquid metal–vapour interface, J. Mater. Sci. 40 (2005) 2133–2140.

[21] D. Chatain, W.C. Carter, Wetting dynamics. Spreading of metallic drops, Nat. Mater. 3 (2004) 843–845.

[22] O. Dezellus, F. Hodaj, N. Eustathopoulos, Chemical reaction-limited spreading: the triple line velocity versus contact angle relation, Acta Mater. 50 (2002) 4741–4753.

[23] P. Xiao, B. Derby, Wetting of TiN and TiC by liquid metals, Acta Mater. 44 (1996) 307–314.

[24] M.L. Muolo, M. Bassoli, B. Wollein, W. Lengauer, A. Passerone, Wetting of TiN by liquid Cu, Trans. J.W.R.I. 30 (2001) 49–54.

[25] D. Chatain, C. Lesueur, J.P. Baland, Wetting of Pb on oxidized micro-patterned Si wafers, Langmuir 22 (2006) 4230–4236.

[26] C. Rado, S. Kalogeropoulou, N. Eustathopoulos, Wetting and adhesion in metal–SiC systems: the effect of surface polarity of SiC, Scripta Mater. 42 (2000) 203–208.

[27] D. Chatain, Anisotropy of wetting, Annu. Rev. Mater. Res. 38 (2008) 45–70.

[28] M.L. Muolo, E. Ferrera, R. Novakovic, A. Passerone, Wettability of zirconium diboride ceramics by Ag, Cu, and their alloys with Zr, Scripta Mater. 48 (2003) 191–196.

[29] G. Kumar, K.N. Prabhu, Review of non-reactive and reactive wetting of liquids on surfaces, Adv. Colloid Interface Sci. 133 (2) (2007) 61–89.

[30] N. Eustathopoulos, Progress in understanding and modeling reactive wetting of metals on ceramics, Curr. Opin. Solid State Mater. Sci. 9 (4–5) (2005) 152–160.

[31] Y.V. Naidich, About liquid metal/ceramic interface interaction mechanism and mode of a new intermediate compound formation, Curr. Opin. Solid State Mater. Sci. 9 (4–5) (2005) 161–166.

[32] E. Saiz, A.P. Tomsia, Kinetics of high-temperature spreading, Curr. Opin. Solid State Mater. Sci. 9 (4–5) (2005) 167–173.

[33] N. Sobczak, M. Singh, R. Asthana, High-temperature wettability measurement in metal/ceramic systems—some methodological issues, Curr. Opin. Solid State Mater. Sci. 9 (4–5) (2005) 241–253.

[34] E. Saiz, A.P. Tomsia, Atomic dynamics and Marangoni films during liquid–metal spreading, Nat. Mater. 3 (12) (2004) 903–909.

[35] K. Kurokawa, R. Nagasaki, Reactivity of sintered SiC with metals, in: S. Somiya, M. Shimada, M. Yoshimura, R. Watanabe (Eds.), Sintering ‘87, Elsevier, New York, 1988, pp. 1397–1402.

[36] B.H. Rabin, A Review of Silicon Carbide/Metal Interactions with Relevance to Silicon Carbide Joining, EG and G Idaho, Inc., Idaho Falls, Washington, 1991, pp. 1–14.

[37] S.J. Li, L. Zhang, Joining SiC-based materials to themselves and metals, Powder Metall. Technol. 22 (2) (2004) 91–97.

[38] T. Fukai, M. Naka, J.C. Schuster, Interfacial structure and reaction mechanism of SiC/V joints, Trans. J.W.R.I. 26 (1) (1997) 93–98.

[39] O. Knacke, O. Kubaschewski, K. Heselmann, Thermochemical Properties of Inorganic Substances, 2nd ed., Springer-Verlag, Berlin, Heidelberg, 1991.

[40] I. Barin, Thermochemical Data of Pure Substances, 3rd ed., WILEY–VCH Verlag GmbH, Weinheim, 1995.

[41] J.G. Li, Wettability of solid inorganic materials by gold, Scripta Metall. Mater. 30 (3) (1994) 337–342.

[42] Y.V. Naidich, V. Zhuravlev, N. Krasovskaya, The wettability of silicon carbide by Au–Si alloys, Mater. Sci. Eng. A 245 (2) (1998) 293–299.

[43] J.G. Li, H. Hausner, Wettability of silicon carbide by gold, germanium and silicon, J. Mater. Sci. Lett. 10 (21) (1991) 1275–1276.

[44] K. Nogi, K. Ogino, Wettability of SiC by liquid pure metals, Trans. Jpn. Inst. Met. 29 (9) (1988) 742–747.

[45] S. Takahashi, O. Kuboi, Study on contact angles of Au, Ag, Cu, Sn, Al and Al alloys to SiC, J. Mater. Sci. 31 (7) (1996) 1797–1802.

[46] M. Shimbo, M. Naka, I. Okamoto, Wettability of silicon carbide by aluminium, copper and silver, J. Mater. Sci. Lett. 8 (66) (1989) 663–666.

[47] J.G. Li, Wettability of silicon carbide by liquid silver and binary silver–silicon alloy, Mater. Lett. 18 (5–6) (1994) 291–298.

[48] S. Kalogeropoulou, C. Rado, N. Eustathopoulos, Mechanisms of reactive wetting: the wetting to non-wetting case, Scripta Mater. 41 (7) (1999) 723–728.

[49] C. Rado, S. Kalogeropoulou, N. Eustathopoulos, Bonding and wetting in non-reactive metal/SiC systems: weak or strong interfaces? Mater. Sci. Eng. A 276 (1–2) (2000) 195–202.

[50] A. Tsoga, S. Ladas, P. Nikolopoulos, Correlation between the oxidation state of α-SiC and its wettability with non-reactive (Sn) or reactive (Ni) metallic components and their binary Si-alloys, Acta Mater. 45 (9) (1997) 3515–3525.

[51] P. Nikolopoulos, S. Agathopoulos, G.N. Angelopoulos, N. Naoumidis, H. Grubmeier, Wettability and interfacial energies in SiC–liquid metal systems, J. Mater. Sci. 27 (1) (1992) 139–145.

[52] B.C. Allen, W.D. Kingery, Surface tension and contact angles in some liquid metal–solid ceramic systems at elevated temperatures, Trans. Met. Soc. AIME 227 (1959) 30–37.

[53] S.J. Li, Y. Zhou, H.P. Duan, Wettability and interfacial reaction in SiC/Ni plus Ti system, J. Mater. Sci. 37 (12) (2002) 2575–2579.

[54] S. Kalogeropoulou, L. Baud, N. Eustathopoulos, Relationship between wettability and reactivity in Fe/SiC system, Acta Metall. Mater. 43 (3) (1995) 907–912.

[55] C. Rado, B. Drevet, N. Eustathopoulos, The role of compound formation in reactive wetting: the Cu/SiC system, Acta Mater. 48 (18–19) (2000) 4483–4491.

[56] G.G. Gnesin, Y.V. Naidich, Contact reaction of silicon carbide with fused copper, Powder Metall. Met. Ceram. 8 (2) (1969) 128–132.

[57] K. Nogi, K. Ogino, Characteristic wettability of SiC by liquid pure Cu, Trans. Jpn. Inst. Met. 29 (10) (1988) 805–811.

[58] C.A. Leon, R.A.L. Drew, The influence of nickel coating on the wettability of aluminum on ceramics, Composites Part A 33 (10) (2002) 1429–1432.

[59] C.A. Leon, G. Mendoza-Suarez, R.A.L. Drew, Wettability and spreading kinetics of molten aluminum on copper-coated ceramics, J. Mater. Sci. 41 (16) (2006) 5081–5087.

[60] D.S. Han, H. Jones, H.V. Atkinson, The wettability of silicon carbide by liquid aluminium: the effect of free silicon in the carbide and of magnesium, silicon and copper alloy additions to the aluminium, J. Mater. Sci. 28 (10) (1993) 2654–2658.

[61] A.C. Ferro, B. Derby, Wetting behaviour in the Al–Si/SiC system interfacial reactions and solubility effects, Acta Metall. Mater. 43 (8) (1995) 3061–3073.

[62] V. Laurent, D. Chatain, N. Eustathopoulos, Wettability of SiC by aluminium and Al–Si alloys, J. Mater. Sci. 22 (1) (1987) 244–250.

[63] V. Laurent, C. Rado, N. Eustathopoulos, Wetting kinetics and bonding of Al and Al alloys on α-SiC, Mater. Sci. Eng. A 205 (1–2) (1996) 1–8.

[64] V.L. Yupko, G.G. Gnesin, Yu.P. Dyban, T.I. Kuzmina, I.E. Polomoshnov, Z.V. Sichkar, The wetting of self-bonded polycrystalline silicon carbide by silicon. II. Effect of surface roughness of the base plate on wetting, Powder Metall. Met. Ceram. 16 (11) (1977) 860–862.

[65] V.L. Yupko, G.G. Gnesin, Yu.P. Dyban, T.I. Kuzmina, I.E. Polomoshnov, Z.V. Sichkar, The wetting of self-bonded polycrystalline silicon carbide by silicon. I. Effect of phase composition on wetting, Powder Metall. Met. Ceram. 16 (10) (1977) 777–780.

[66] C. Rado, S. Kalogeropoulou, N. Eustathopoulos, Wetting and adhesion in metal–silicon carbide systems: the effect of surface polarity of SiC, Scripta Mater. 42 (2) (2000) 203–208.

[67] T.J. Whalen, A.T. Andersson, Wetting of SiC, Si_3N_4, and carbon by Si and binary Si alloys, J. Am. Ceram. Soc. 58 (9–10) (1975) 396–399.

[68] M. Syvajarvi, R. Yakimova, E. Janzen, Growth of SiC from the liquid phase: wetting and dissolution of SiC, Diamond Relat. Mater. 6 (10) (1997) 1266–1268.

[69] Z. Yuan, W.L. Huang, K. Mukai, Wettability and reactivity of molten silicon with various substrates, Appl. Phys. A 78 (4) (2004) 617–622.

[70] J.A. Champion, B.J. Keene, S. Allen, Wetting of refractory materials by molten metallides, J. Mater. Sci. 8 (3) (1973) 423–426.

[71] R. Warren, C.H. Anderson, Silicon carbide fibres and their potential for use in composite materials. Part II, Composites 15 (2) (1984) 101–111.

[72] L.D. Lucas, Données physico-chimiques des principaux métaux et métalloïdes, vol. MB2, Techniques de l'Ingénieur, Paris, M65, 1984, pp. 1–14.

[73] B.C. Allen, The surface tension of liquid metals, in: S.Z. Beer (Ed.), Liquid Metals: Chemistry and Physics, Marcel Dekker Inc., New York, 1972, pp. 161–212.

[74] H. Fujii, T. Matsumoto, S. Izutani, S. Kiguchi, K. Nogi, Surface tension of molten silicon measured by microgravity oscillating drop and improved sessile drop method, Acta Mater. 54 (2006) 1221–1225.

[75] Y.V. Naidich, V.M. Perevertailo, L.P. Obushchak, Density and surface tension of alloys of the systems Au–Si and Au–Ge, Poroshkovaya Metall. 149 (5) (1975) 73–75.

[76] R.C. Weast, Handbook of Chemistry and Physics, 55th ed., CRC Press, Cleveland, 1974.

[77] P. Nikolopoulos, G. Ondracek, D. Sotiropoulou, Wettability and interfacial energies between zirconia ceramic and liquid metals, Ceram. Int. 15 (1989) 201–206.

[78] J.G. Li, H. Hausner, Contact angle and work of adhesion isotherms of silicon–tin alloys on monocrystalline silicon carbide, Mater. Lett. 11 (10–12) (1991) 355–357.

[79] P. Nikolopoulos, D. Sotiropoulou, Wettability between zirconia ceramics and the liquid metals copper, nickel and cobalt, J. Mater. Sci. Lett. 6 (12) (1987) 1429–1430.

[80] F. Xiao, L. Fang, K. Nogi, Surface tension of molten Ni and Ni–Co alloys, J. Mater. Sci. Technol. 21 (2) (2005) 201–206.

[81] K.C. Mills, Y.C. Su, Review of surface tension data for metallic elements and alloys. Part 1. Pure metals, Int. Mater. Rev. 51 (2006) 329–351.

[82] C. Rado, Contribution to the study of wetting and thermodynamic adhesion of liquid metals and alloys on silicon carbide, Ph.D. Thesis, INP Grenoble, France, 1997.

[83] X.B. Zhou, J.Th.M. De Hosson, Reactive wetting of liquid metals on ceramic substrates, Acta Mater. 44 (2) (1996) 421–426.

[84] I. Lauermann, F. Sauerwald, Surface tensions of molten copper, silver, antimony, and copper–tin, copper–antimony, and silver–antimony alloys, Z, Metatlk 55 (10) (1964) 605–612.

[85] V.L. Yupko, Wetting of silicon carbide by Cu–Ti and Cu–Sn–Ti alloys, Powder Metall. Met. Ceram. 16 (9) (1977) 718–720.

[86] P.F. Paradis, T. Ishikawa, N. Koike, Thermophysical property measurements of liquid and supercooled cobalt, High Temp. High Press. 37 (1) (2008) 5–11.

[87] B.J. Keene, Review of data for surface-tension of pure metals, Int. Mater. Rev. 38 (4) (1993) 157–192.

[88] M. Humenik Jr., W.D. Kingery, Metal–ceramic interactions. III. Surface tension and wettability of metal–ceramic systems, J. Am. Ceram. Soc. 37 (1) (1954) 18–23.

[89] N. Eustathopoulos, B. Drevet, E. Ricci, Temperature coefficient of surface tension for pure liquid metals, J. Cryst. Growth 191 (1–2) (1998) 268–274.

[90] N. Eustathopoulos, E. Ricci, B. Drevet, Tension superficielle, Techniques de l'Ingenieur 3 (1999), M67-1-13.

[91] L.E. Murr, Intefacial Phenomena in Metals and Alloys, Addison-Wesley, London, 1975, pp. 108–111.

[92] N. Eustathopoulos, A. Passerone, On the calculation of solid–liquid interfacial tension in metallic systems from contact angle data, J. Mater. Sci. Lett. 2 (1983) 197–200.

[93] R.H. Bruce, Aspects of the surface free energies, in: G.H. Stewart (Ed.), Science of Ceramics, Academic Press, London, 1965, pp. 359–381.

[94] B.N. Oshcherin, On surface energies of $A^{N}B^{8-N}$ semiconducting compounds, Phys. Stat. Solidi A 34 (2) (1976) K181–K182.

[95] T. Takai, T. Halicioglu, W.A. Tiller, Reconstruction and energetics for surfaces of silicon, diamond and β-SiC, Surf. Sci. 164 (2–3) (1985) 341–352.

[96] B. Drevet, S. Kalogeropoulou, N. Eustathopoulos, Wettability and interfacial bonding in Au–Si/SiC system, Acta Metall. Mater. 41 (11) (1993) 3119–3126.

[97] Y. Du, J.C. Schuster, Experimental investigation and thermodynamic descriptions of the Ni–Si and C–Ni–Si systems, Metall. Mater. Trans. 30 (1999) 2409–2418.

[98] G.W. Liu, F. Valenza, M.L. Muolo, G.J. Qiao, A. Passerone, J. Mater. Sci. 44 (22) (2009) 5590–5597.

[99] A. Gasse, G. Chaumat, C. Rado, N. Eustathopoulos, Influence of atmosphere on the wettability of α-SiC by non-reactive Cu–Si alloys, J. Mater. Sci. 15 (8) (1996) 1630–1632.

[100] K. Landry, C. Rado, N. Eustathopoulos, Influence of interfacial reaction rates on the wetting driving force in metal/ceramic systems, Metall. Mater. Trans. A 27 (10) (1996) 3181–3186.

[101] C. Rado, N. Eustathopoulos, The role of surface chemistry on spreading kinetics of molten silicides on silicon carbide, Interface Sci. 12 (1) (2004) 85–92.

[102] P. Xiao, B. Derby, Wetting of silicon carbide by chromium containing alloys, Acta Mater. 46 (10) (1998) 3491–3499.

[103] O. Mailliart, F. Hodaj, V. Chaumat, N. Eustathopoulos, Influence of oxygen partial pressure on the wetting of SiC by a Co–Si alloy, Mater. Sci. Eng. A 495 (1–2) (2008) 174–180.

[104] A.E. Mattsson, P.A. Schultz, M.P. Desjarlais, T.R. Mattsson, K. Leung, Designing meaningful density functional theory calculations in materials science—a primer, Modell. Simul. Mater. Sci. Eng. 13 (1) (2005) R1–R31.

[105] X.G. Wang, J.R. Smith, Adhesion of copper and alumina from first principles, J. Am. Ceram. Soc. 86 (4) (2003) 696–700.

[106] W. Zhang, J.R. Smith, Nonstoichiometric interfaces and Al_2O_3 adhesion with Al and Ag, Phys. Rev. Lett. 85 (15) (2000) 3225–3228.

[107] M.W. Finnis, The theory of metal–ceramic interfaces, J. Phys. Condens. Matter 8 (32) (1996) 5811–5836.

[108] S.P. Mehandru, A.B. Anderson, Adhesion and bonding of polar and nonpolar SiC surfaces to Ti(0 0 0 1), Surf. Sci. 245 (1991) 333–344.

[109] M.L. Liu, S.Q. Wang, H.Q. Ye, First-principles study of metal/nitride polar interfaces: Ti/TiN, Surf. Interf. Anal. 35 (2003) 835–841.

[110] C. Hashibon, M. Elsässer, Rühle, Ab-initio study of electronic densities of states at Cu/alumina interfaces, Acta Mater. 55 (2007) 1657–1665.